Molecules and Cells

Overexpression and Selective Anticancer Efficacy of *ENO3* in *STK11* Mutant Lung Cancers

Choa Park[1,3], Yejin Lee[1,3], Soyeon Je[1,3], Shengzhi Chang[1], Nayoung Kim[1], Euna Jeong[2], and Sukjoon Yoon[1,2,*]

[1]Department of Biological Sciences, Sookmyung Women's University, Seoul 04310, Korea, [2]Research Institute of Women's Health, Sookmyung Women's University, Seoul 04310, Korea, [3]These authors contributed equally to this work.
*Correspondence: yoonsj@sookmyung.ac.kr
https://doi.org/10.14348/molcells.2019.0099
www.molcells.org

Oncogenic gain-of-function mutations are clinical biomarkers for most targeted therapies, as well as represent direct targets for drug treatment. Although loss-of-function mutations involving the tumor suppressor gene, *STK11 (LKB1)* are important in lung cancer progression, *STK11* is not the direct target for anticancer agents. We attempted to identify cancer transcriptome signatures associated with *STK11* loss-of-function mutations. Several new sensitive and specific gene expression markers (*ENO3, TTC39C, LGALS3,* and *MAML2*) were identified using two orthogonal measures, i.e., fold change and odds ratio analyses of transcriptome data from cell lines and tissue samples. Among the markers identified, the *ENO3* gene over-expression was found to be the direct consequence of *STK11* loss-of-function. Furthermore, the knockdown of *ENO3* expression exhibited selective anticancer effect in *STK11* mutant cells compared with *STK11* wild type (or recovered) cells. These findings suggest that *ENO3*-based targeted therapy might be promising for patients with lung cancer harboring *STK11* mutations.

Keywords: *Enolase 3*, lung adenocarcinoma, *STK11* loss-of-function mutation

INTRODUCTION

Non-small-cell lung carcinoma (NSCLC) is a type of epithelial lung cancer, constituting ~80% to 90% of all lung cancers (Novello et al., 2016; Planchard et al., 2018). NSCLC is classified into three types: lung adenocarcinoma (LUAD), squamous cell carcinoma, and large cell carcinoma. LUAD accounts for approximately 30% of lung cancers (Gill et al., 2011). *Serine/threonine kinase 11* (*STK11*), also known as *liver kinase B1* (*LKB1*), is a major tumor suppressor gene in lung cancers. Particularly, *STK11* is the most inactivated tumor suppressor gene in NSCLC (Carretero et al., 2004; Chen et al., 2016; Facchinetti et al., 2017). Although *STK11* inactivation (i.e., loss-of-function mutation) occurs in ~30% of LUAD (Kim et al., 2016), its role in cancer progression has yet to be elucidated (Gao et al., 2010).

In previous studies, we found target genes and drugs with *STK11* mutation-specific anticancer efficacy in lung cancer cell lines (He et al., 2014; Kim et al., 2016). The expression of *phosphodiesterase-4D* (*PDE4D*) was found to be upregulated in both lung cancer cell lines and tissue samples harboring *STK11* homogeneous mutations. Knockdown of *PDE4D* gene expression and chemical inhibition of *PDE4D* protein enhanced the anticancer efficacy in *STK11*-mutant cell lines compared with other lung cancer cell lines (He et al., 2014). Drugs inhibiting *ATPase Na+/K+ Transporting Subunit Alpha 1* (*ATP1A1*) also showed selective efficacy in *STK11*-mutant lung cancer cell lines (Kim et al., 2016). In the present study, we systematically analyzed the cancer transcriptome to further identify *STK11*-specific gene expression signatures in

Received 20 May, 2019; revised 2 October, 2019; accepted 13 October, 2019; published online 7 November, 2019

eISSN: 0219-1032

lung cancers. We compared the gene expression profile of *STK11* loss-of-function cells (homozygous mutations) and *STK11* wild type cells from the LUAD cell line panel and tissue samples. The expression of several genes exhibited significant sensitivity and specificity to the *STK11* mutation. Particularly, the expression of *Enolase 3* (*ENO3*) was altered by the loss or recovery of *STK11* gene expression.

Enolase (*ENO*), also known as phosphopyruvate dehydratase, is a metalloenzyme that catalyzes the transformation of *2-phosphoglycerate* (2-PG) to *phosphoenolpyruvate* (PEP) during glycolysis (Ho et al., 2010). The three isoforms of *ENO*s in mammalian cells include: α or *non-neuronal enolase* (*NNE*), γ or *neuron-specific enolase* (*NSE*), and β or *muscle-specific enolase* (*MSE*) (Muller et al., 2012; Peshavaria and Day, 1991). They are cytoplasmic enzymes involved in glycolysis and gluconeogenesis (Lung et al., 2017). Specially, the expression of *ENO1* was highlighted in small-cell lung carcinoma (SCLC) tissues, suggesting its association with cancer cell migration (Ho et al., 2010; Liu and Shih, 2007). The increased expression of *ENO2* gene has also been reported in NSCLC (Ho et al., 2010; Isgrò et al., 2015). However, the role and function of *ENO3* in cancer have yet to be elucidated. Here, we present the results of *ENO3* regulation by the *STK11* gene expression via *STK11* mutation-specific transcriptome analysis. The therapeutic potential of *ENO3* as the *STK11* mutation-specific target was also investigated. This study extends our knowledge of *STK11* mutation-driven cancer progress, and contributes to the development of new targeted therapies.

MATERIALS AND METHODS

Data acquisition

DNA microarray gene expression data of 47 LUAD cell lines were obtained from the Cancer Cell Line Encyclopedia (CCLE) (Barretina et al., 2012). mRNA expression levels obtained using Affymetrix U133 plus 2.0 arrays were represented as $\log_2$-transformed value after robust multichip average (RMA) normalization. The expression ranges are from 3 to 15 and the average expression is 7.5. Among 54,613 gene probes, the data available for the 15,080 gene probes in > 50% of selected LUAD cell lines were used in the present analysis. *STK11* loss-of-function cell lines were defined by analyzing the accompanying exome sequencing data (Supplementary Table 1). For the analysis of *STK11*-dependent gene expression, we retrieved the DNA microarray data of two *STK11* mutant, parental A549 cell lines and two *STK11*-recovered A549 cell lines (GSE6135) from Gene Expression Omnibus (GEO; http://www.ncbi.nlm.nih.gov/geo/) (Clough and Barrett, 2016). Gene expression data were obtained using Agilent Homo sapiens 44k custom array and represented as $\log_2$ scale after normalization by locally weighted scatterplot smoothing (LOWESS). In addition, 230 patient tissue-based gene expression and exome sequencing data of LUAD were obtained from The Cancer Genome Atlas (TCGA) (Cancer Genome Atlas Research Network et al., 2013). The RNA-seq expression level of each gene was represented with $\log_2$-transformed through upper quartile normalized RSEM (RNA-Seq by Expectation Maximization).

Sensitivity and specificity

To identify differentially expressed genes between *STK11* mutant and wild-type cell lines, we used fold change and *t*-test *P* values. The fold change is defined as the difference between the averages of two compared groups. For statistical significance, we calculated *P* values from the *t*-statistic. To determine the selective association between gene expression and *STK11* mutation, we also calculated the enrichment score using the odds ratio between the observed odds and the expected odds. The observed and the expected odds are defined as the ratio of cell lines with over threshold (fold change > 1) among *STK11* mutant LUAD and among all LUAD cell lines, respectively. The statistical confidence of an odds ratio was calculated using Fisher's exact test. Statistical analysis was performed using Perl (ver. 5.30.0; http://www.perl.org/).

Cell-based *in vitro* assays

A549, H23, H1993, and H322M cells were obtained from the National Institutes of Health, National Cancer Institute (NCI, USA). HCC-827 and H1975 cells were obtained from the American Type Culture Collection (ATCC, USA). The *STK11*-recovered cells from three parental cell lines (A549-*STK11*, H23-*STK11*, and H1993-*STK11*) were established in our laboratory (Kim et al., 2016). *STK11* mutant and wild-type cell lines were cultured in RPMI 1640 (HyClone Laboratories, USA) supplemented with 10% fetal bovine serum (HyClone Laboratories) and 1% antibiotics (Thermo Fisher Scientific, USA) according to institutional laboratory safety guidelines. The *STK11*-recoverd cell lines were cultured in the same medium after supplementation with 1 μg/ml puromycin. The cells were maintained at 37°C in a 5% CO_2 incubator and subcultured at 80% to 90% confluence. The media were changed every 2 to 3 days. A total of 1 to 3 × 10^5 cells per well were seeded on a 6-well culture plate for monolayer cell cultures for 3 days.

For siRNA transfection, we experimented with 10 nmol/L target siRNAs of NC (negative control), PLK1 (positive control), and *ENO3* (Thermo Fisher Scientific, On-Target Plus SmartPool; GE Dharmacon, USA) (Song et al., 2017). Cells were seeded in a 96-well plate (Corning, USA) at an optimized density of 2,000 to 8,000 cells/well. After 72 h of seeding, the viability was measured using the CellTiter-Blue for Cell Viability Assay (Promega, USA). Simultaneously, cells were stained with DAPI and single cells were counted with Gen5™ software (BioTek Instruments, USA).

Quantitative real-time polymerase chain reaction analysis

Total RNA was extracted in 6-well plates using TRIzol. Synthesis of cDNA and polymerase chain reaction (PCR) amplification were carried out with the SuperScript One-step RT-PCR Platinum Taq Kit (Invitrogen, USA). The gene expression of *ENO1*, *ENO2*, and *ENO3* was quantified via real-time PCR using specific primer sets targeting *ENO1* (Hs00157360_m1, TaqMan), *ENO2* (Hs00361415_m1, TagMan), and *ENO3* (Hs01093275_m1, TaqMan), respectively, and the reference gene *GAPDH* (Hs02786624_g1, TagMan) (Ali et al., 2015; Liu et al., 2005). Quantitative real-time PCR (RT-qPCR) were carried out on an Applied Biosystems 7500 (Thermo Fisher

Scientific) using a TaqMan real-time detection protocol. The delta cycle threshold (dCt) corresponds to the cycle threshold (Ct) values for *ENO1*, *ENO2*, and *ENO3* RNA expression normalized to those for RNA expression of the internal control *GAPDH*. For intuitive interpretation, -dCt is used so as that the higher values indicate a higher normalized target gene expression.

RESULTS AND DISCUSSION

Analysis of *STK11*-associated gene expression in LUAD cell lines

DNA microarray data of 47 LUAD cell lines were analyzed to identify the gene expression markers associated with *STK11* mutations (Fig. 1). We compared the differences in gene expression between nine cell lines with *STK11* loss-of-function mutations (Supplementary Table 1) and 38 *STK11* wild-type cell lines based on fold change and odds ratio. The fold change reflects the sensitivity of the gene expression in *STK11* mutant cells against *STK11* wild-type cells, while the odds ratio quantifies the specificity (i.e., exclusiveness) of a gene expression in *STK11*-mutant cell lines compared with other cell lines (see Materials and Methods section for details). As a result, 222 gene probes (sensitive hits) were significantly ($P < 0.01$) over- or under-expressed (> 2-fold change) in *STK11* mutation cells in LUAD, while the expression of 71 gene probes (specific hits) exhibited significantly ($P < 0.01$) exclusive expression (> 2-odds ratio). Since no general correlation was observed between sensitivity and specificity of gene expression, the selection of common hits based on these two measures provided unique gene expression signatures (or biomarkers) of *STK11* mutant cancer cells. A total of 11 gene probes satisfied both sensitivity and specificity of the expression associated with *STK11* loss-of-function mutations (Fig. 1). These 11 genes were identified from diverse functional classes and their functional or signaling aspects have never been reported in connection with the suppressive role of *STK11* in the cancer progression.

We further investigated the association of these 11 gene expression profiles associated with *STK11* mutations using the RNA sequencing data of patient-derived tumor tissue samples. The gene expression was statistically compared between 40 *STK11*-mutant and 190 wild-type LUAD samples from the TCGA database (see Materials and Methods section). Among the 11 genes selected from the analysis of cell line data in Figure 1, the expression of *ENO3* and *TTC39C* genes was found to be significantly up-regulated in *STK11* mutant tissue samples (Fig. 2A). Down-regulation of *LGALS3* and *MAML2* genes in *STK11*-mutant cell lines was also confirmed in patient-derived LUAD samples. Particularly, the differential expression of the *ENO3* gene in *STK11*-mutant and wild type samples was greater than 2-fold in tissue samples, displaying a minimal level of the *ENO3* gene expression in most of the *STK11* wild-type LUAD samples.

STK11-dependent *ENO3* gene expression

The gene expression of *ENO3*, *TTC39C*, *LGALS3*, and *MAML2* was consistently up-or down-regulated in both *STK11*-mutant cell lines and tissue samples of LUAD. We thus investigated the changes in their gene expression based on the recovery of *STK11* function in the *STK11*-mutant LUAD cell line (A549). DNA microarray data of *STK11*-mutant (loss-of-function) A549 and *STK11*-recovered A549 cell lines were retrieved from the GEO database (GSE6135). Since the gene expression data of *TTC39C* were not available in the dataset, we only analyzed the differential expression of *ENO3*, *LGALS3*, and *MAML2* in *STK11*-mutant and *STK11*-recovered A549 cells (Fig. 2B). While the expression of *LGALS3* and *MAML2* was not changed by *STK11* functional recovery, the *ENO3* expression was greatly reduced in *STK11*-recovered A549 cells compared with *STK11*-mutant A549 cells suggesting that the *ENO3* over-expression in both *STK11*-mutant

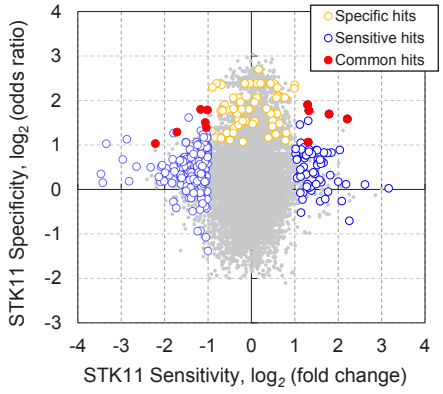

	Gene	Probe ID	Full name
Up-regulated	ANKRD55	240456_at	Ankyrin repeat domain 55
	ENO3	204483_at	Enolase 3 (beta, muscle)
	FDXR	207813_s_at	Ferredoxin reductase
	GNAL	206355_at	Guanine nucleotide binding
	TTC39C	238480_at	Tetratricopeptide repeat domain 39C
Down-regulated	C9orf95	219147_s_at	Chromosome 9 open reading frame 95
	FAM111A	218248_at	Family with sequence similarity 111, member A
	LGALS3	208949_s_at	Lectin, galactoside-binding, soluble, 3
	MAML2	235457_at	Mastermind-like transcriptional coactivator 2
	SHROOM3	225548_at	Shroom family member 3
	TMEM54	225536_at	Transmembrane protein 54

Fig. 1. Analysis of gene expression associated with *STK11* mutations. A total of 15,080 gene probes were plotted to determine *STK11* sensitive vs. *STK11* specific expression in the CCLE dataset. The sensitivity (i.e., $\log_2$ fold-change) was determined based on the gene expression ratio in nine *STK11*-mutant cell lines compared with 38 *STK11* wild-type cell lines. The specificity (i.e., $\log_2$ odds ratio) of a gene expression was based on the ratio of the observed odds in *STK11*-mutant cell lines over the expected odds in all cell lines. Orange circles represent the 71 *STK11*-specific gene probes with > 2 odds ratio (Fisher's exact test, $P < 0.01$) in *STK11*-mutant cell lines. Blue circles represent the 222 *STK11*-sensitive gene probes with > 2 fold change (Student's *t*-test, $P < 0.01$) in *STK11*-mutant cell lines. Filled red circles represent 11 common hits of specific (orange) and sensitive (blue) gene probes.

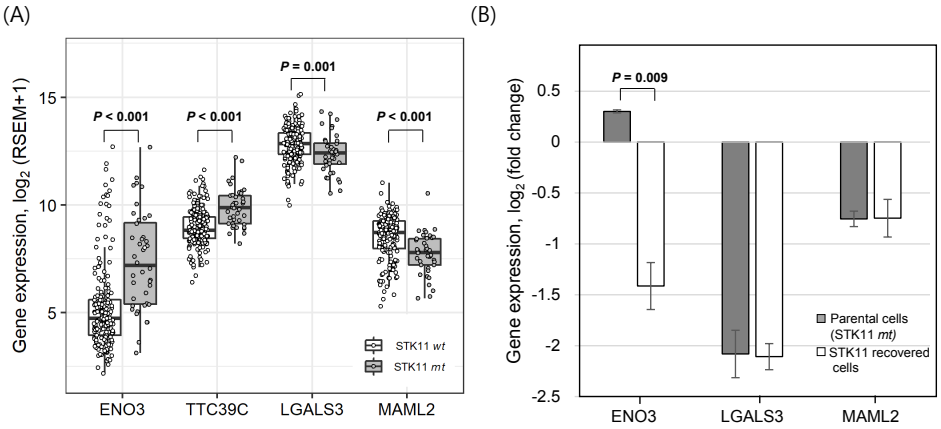

Fig. 2. *STK11*-specific expression of selected genes in LUAD tissue samples and *STK11*-recovered model cell line. (A) Differential expression of genes plotted using LUAD tissue samples retrieved from TCGA. A total of 230 samples were classified into *STK11* mutants (40 samples) and wild types (190 samples), and their gene expression (log_2-transformed upper quartile values) was analyzed. Student's *t*-test for LGALS3 and Wilcoxon rank-sum test for others were used to test statistical significance. (B) Differential gene expression was analyzed in *STK11*-mutant A549 cells and *STK11*-recovered A549 cells retrieved from GEO (GSE6135). Student's *t*-test was used to test statistical significance. Error bars indicate SD.

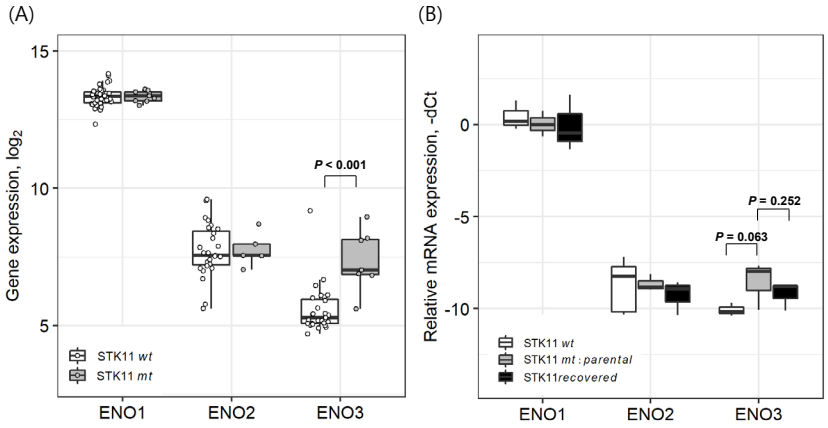

Fig. 3. Expression of ENO gene family in DNA microarray data and qPCR experiment using LUAD cell lines. (A) Comparison of *ENO* family gene expression (ENO1: 201231_s_at, ENO2: 201313_at, and ENO3: 204483_at) between nine *STK11*-mutant and 38 *STK11* wild-type cell lines in the CCLE dataset. Wilcoxon rank-sum test for ENO3 and Student's *t*-test for others were used to test statistical significance. (B) Experimental validation (qPCR) of *ENO* family gene expression in *STK11* wide-type cell lines (H322M, HCC827, and H1975), *STK11*-mutant parental cell lines (A549, H23, and H1993) and *STK11*-restored cell lines. The expression level of GAPDH was observed to be varied within SD < 1 among 9 cell lines. Student's *t*-test was used to test statistical significance. Error bars indicate SD.

LUAD cell lines and tissue samples was a direct the consequence of *STK11* loss-of-function.

Although *ENO1* and *ENO2* have been widely studied in cancer context (Ho et al., 2010; Isgrò et al., 2015; Liu and Shih, 2007), the role of *ENO3* in cancers has yet to be fully elucidated. In our analysis of CCLE dataset, the expression of *ENO1* and *ENO2* did not show any difference between *STK11*-mutant and -wild type cell lines (Fig. 3A). To further confirm the exclusive dependence of *ENO3* overexpression on *STK11* loss-of-function, we measured the mRNA levels of *ENO1*, *ENO2*, and *ENO3* in diverse cell lines with/without *STK11* function (Fig. 3B). As a result, only the expression of *ENO3* exhibited exclusive sensitivity to *STK11* functional status. In these qPCR experiments, cell lines harboring *STK11* mutations (A549, H23, and H1993) displayed > 2-fold overexpression of the *ENO3* mRNAs compared with *STK11* wild-type cell lines (H322M, HCC827, and H1975). Recovery of *STK11* function by the three *STK11*-mutant cell lines reduced the *ENO3* gene expression, although the statistical significance was relatively weak (Fig. 3B). These qPCR validations strongly suggested that *STK11* loss-of-function mutation directly induced the overexpression of *ENO3* in LUAD cells.

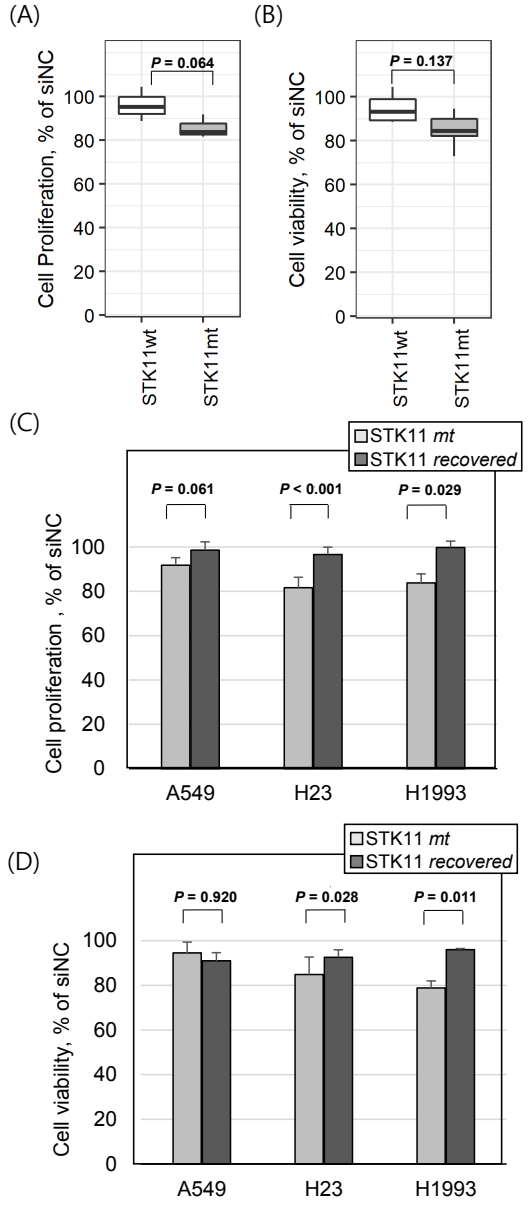

Fig. 4. *STK11* mutation-dependent anticancer efficacy of *ENO3* gene knockdown. Average variation in cell proliferation (A) and cell viability (B) of *STK11* wild-type cell lines (H322M, HCC827, and H1975) and mutant cell lines (A549, H23, and H1993) by the *ENO3* gene knockdown using siRNAs. Comparative changes in cell proliferation (C) and cell viability (D) in *STK11*-mutant parental cells and *STK11* recovered cells by the *ENO3* gene knockdown. Cell proliferation was measured based on the direct cell count in the well. Cell viability was measured using CellTiter Blue assay (see the Materials and Methods section for detail). All y-axes represent percentage of cell proliferation or cell viability divided by an average of negative control. Student's one-tailed *t*-test was used to test statistical significance. Error bars indicate SD.

Selective anticancer effect of *ENO3* knockdown on *STK11*-mutant cancer cells

The observation of *ENO3* overexpression under *STK11* loss-of-function mutations implies that *ENO3* might be a selective anticancer target in *STK11*-mutant cancer. We thus investigated the anticancer effect of *ENO3* knockdown by siRNAs. In case of *STK11* wild-type LUAD cell lines (H322M, HCC827, and H1975), the siENO3 treatment resulted in less than 5% inhibition of cell proliferation in 72 h *in vitro* assays (Fig. 4A). However, the anti-proliferative effect of siENO3 was increased on *STK11*-mutant cell lines (A549, H23, and H1993). The cell viability results were consistent with the cell proliferation assay (Fig. 4B). The viability of *STK11*-mutant cells was more sensitive to siENO3 treatment than *STK11* wild-type cells. We further compared the efficacy of siENO3 in *STK11*-mutant cell lines compared with the corresponding cell lines with *STK11* functional recovery (Figs. 4C and 4D). In both of cell proliferation and viability measures, STK11-recovered cells were less sensitive to siENO3 treatment than the parental mutant cells in H23 and H1993 cases. However, A549 cells showed inconsistent patterns between cell proliferation and viability assays, implying the existence of a cell line-specific effect of the STK11 recovery in cancer cells. Overall, these results in Figure 4 suggest that *ENO3*, induced by *STK11* loss-of-function, might play a selective role in the development of targeted therapies against LUAD cell lines carrying *STK11* mutations as an effective clinical biomarker.

Note: Supplementary information is available on the Molecules and Cells website (www.molcells.org).

Disclosure

The authors have no potential conflicts of interest to disclose.

ACKNOWLEDGMENTS

This work was financially supported by grants from the National Research Foundation of Korea (KRF), including the Science Research Center Program (NRF-2016R1A5A1011974), and the Mid-career Researcher Program (NRF-2017R1A2B2007745 and NRF-2018R1A2B6009313), funded by the Korean government (MEST). This research was also financially supported by the Sookmyung Women's University BK21 Plus Scholarship.

ORCID

Choa Park https://orcid.org/0000-0001-6437-9767
Yejin Lee https://orcid.org/0000-0002-8110-9221
Soyeon Je https://orcid.org/0000-0002-9955-493X
Shengzhi Chang https://orcid.org/0000-0002-9051-7569
Nayoung Kim https://orcid.org/0000-0003-3202-750X
Euna Jeong https://orcid.org/0000-0002-8802-4140
Sukjoon Yoon https://orcid.org/0000-0001-7885-7117

REFERENCES

Ali, H., Du, Z., Li, X., Yang, Q., Zhang, Y.C., Wu, M., Li, Y., and Zhang, G. (2015). Identification of suitable reference genes for gene expression studies using quantitative polymerase chain reaction in lung cancer in vitro. Mol. Med. Rep. *11*, 3767-3773.

Barretina, J., Caponigro, G., Stransky, N., Venkatesan, K., Margolin, A.A., Kim, S., Wilson, C.J., Lehar, J., Kryukov, G.V., Sonkin, D., et al. (2012). The Cancer Cell Line Encyclopedia enables predictive modelling of anticancer drug sensitivity. Nature *483*, 603-607.

Cancer Genome Atlas Research Network, Weinstein, J.N., Collisson, E.A., Mills, G.B., Shaw, K.R., Ozenberger, B.A., Ellrott, K., Shmulevich, I., Sander, C., and Stuart, J.M. (2013). The Cancer Genome Atlas Pan-cancer analysis project. Nat. Genet. *45*, 1113-1120.

Carretero, J., Medina, P.P., Pio, R., Montuenga, L.M., and Sanchez-Cespedes, M. (2004). Novel and natural knockout lung cancer cell lines for the LKB1/STK11 tumor suppressor gene. Oncogene *23*, 4037-4040.

Chen, L., Engel, B.E., Welsh, E.A., Yoder, S.J., Brantley, S.G., Chen, D.T., Beg, A.A., Cao, C., Kaye, F.J., Haura, E.B., et al. (2016). A sensitive NanoString-based assay to score STK11 (LKB1) pathway disruption in lung adenocarcinoma. J. Thorac. Oncol. *11*, 838-849.

Clough, E. and Barrett, T. (2016). The gene expression omnibus database. In Statistical Genomics, E. Mathé and S. Davis, eds. (New York: Humana Press), pp. 93-110.

Facchinetti, F., Bluthgen, M.V., Tergemina-Clain, G., Faivre, L., Pignon, J.P., Planchard, D., Remon, J., Soria, J.C., Lacroix, L., and Besse, B. (2017). LKB1/STK11 mutations in non-small cell lung cancer patients: descriptive analysis and prognostic value. Lung Cancer *112*, 62-68.

Gao, Y., Xiao, Q., Ma, H., Li, L., Liu, J., Feng, Y., Fang, Z., Wu, J., Han, X., Zhang, J., et al. (2010). LKB1 inhibits lung cancer progression through lysyl oxidase and extracellular matrix remodeling. Proc. Natl. Acad. Sci. U. S. A. *107*, 18892-18897.

Gill, R.K., Yang, S.H., Meerzaman, D., Mechanic, L.E., Bowman, E.D., Jeon, H.S., Roy Chowdhuri, S., Shakoori, A., Dracheva, T., Hong, K.M., et al. (2011). Frequent homozygous deletion of the LKB1/STK11 gene in non-small cell lung cancer. Oncogene *30*, 3784-3791.

He, N., Kim, N., Song, M., Park, C., Kim, S., Park, E.Y., Yim, H.Y., Kim, K., Park, J.H., and Kim, K.I. (2014). Integrated analysis of transcriptomes of cancer cell lines and patient samples reveals STK11/LKB1-driven regulation of cAMP phosphodiesterase-4D. Mol. Cancer Ther. *13*, 2463-2473.

Ho, J.A., Chang, H.C., Shih, N.Y., Wu, L.C., Chang, Y.F., Chen, C.C., and Chou, C. (2010). Diagnostic detection of human lung cancer-associated antigen using a gold nanoparticle-based electrochemical immunosensor. Anal. Chem. *82*, 5944-5950.

Isgrò, M.A., Bottoni, P., and Scatena, R. (2015). Neuron-specific enolase as a biomarker: biochemical and clinical aspects. In Advances in Cancer Biomarkers, R. Scatena, ed. (Dordrecht, The Netherlands: Springer), pp. 125-143.

Kim, N., Yim, H.Y., He, N., Lee, C.J., Kim, J.H., Choi, J.S., Lee, H.S., Kim, S., Jeong, E., and Song, M. (2016). Cardiac glycosides display selective efficacy for STK11 mutant lung cancer. Sci. Rep. *6*, 29721.

Liu, D.W., Chen, S.T., and Liu, H.P. (2005). Choice of endogenous control for gene expression in nonsmall cell lung cancer. Eur. Respir. J. *26*, 1002-1008.

Liu, K.J. and Shih, N.Y. (2007). The role of enolase in tissue invasion and metastasis of pathogens and tumor cells. J. Cancer Mol. *3*, 45-48.

Lung, J., Chen, K.L., Hung, C.H., Chen, C.C., Hung, M.S., Lin, Y.C., Wu, C.Y., Lee, K.D., Shih, N.Y., and Tsai, Y.H. (2017). In silico-based identification of human α-enolase inhibitors to block cancer cell growth metabolically. Drug Des. Devel. Ther. *11*, 3281-3290.

Muller, F.L., Colla, S., Aquilanti, E., Manzo, V.E., Genovese, G., Lee, J., Eisenson, D., Narurkar, R., Deng, P., and Nezi, L. (2012). Passenger deletions generate therapeutic vulnerabilities in cancer. Nature *488*, 337-342.

Novello, S., Barlesi, F., Califano, R., Cufer, T., Ekman, S., Levra, M.G., Kerr, K., Popat, S., Reck, M., Senan, S., et al. (2016). Metastatic non-small-cell lung cancer: ESMO Clinical Practice Guidelines for diagnosis, treatment and follow-up. Ann. Oncol. *27*(Suppl 5), v1-v27.

Peshavaria, M. and Day, I.N. (1991). Molecular structure of the human muscle-specific enolase gene (ENO3). Biochem. J. *275*, 427-433.

Planchard, D., Popat, S., Kerr, K., Novello, S., Smit, E.F., Faivre-Finn, C., Mok, T.S., Reck, M., Van Schil, P.E., Hellmann, M.D., et al. (2018). Metastatic non-small cell lung cancer: ESMO Clinical Practice Guidelines for diagnosis, treatment and follow-up. Ann. Oncol. *29*(Suppl 4), iv192-iv237.

Song, M., Lee, H., Nam, M.H., Jeong, E., Kim, S., Hong, Y., Kim, N., Yim, H.Y., Yoo, Y.J., Kim, J.S., et al. (2017). Loss-of-function screens of druggable targetome against cancer stem-like cells. FASEB J. *31*, 625-635.